Clays and Clay Minerals, Vol. 47, No. 6, 748–754, 1999.

FORMATION OF GOETHITE AND HEMATITE FROM NEODYMIUM-CONTAINING FERRIHYDRITE SUSPENSIONS

TETSUSHI NAGANO,[1,†] HISAYOSHI MITAMURA,[1,†] SHINICHI NAKAYAMA,[1,‡] AND SATORU NAKASHIMA[2,§]

[1] Department of Environmental Safety Research, Japan Atomic Energy Research Institute, Tokai, Naka, Ibaraki 319-1195, Japan

[2] Department of Earth and Planetary Materials Science, Graduate School of Science, Hokkaido University, N10 W8, Sapporo 060-0810, Japan

Abstract—The effects of neodymium (Nd) on the transformation of ferrihydrite to iron oxides was studied. The possible isomorphous substitution of Nd^{3+} for Fe^{3+} in iron oxides was examined also. Nd was used as an inactive substitute of trivalent radioactive actinide elements. Hydrolysis of ferric nitrate solution containing 0–30 mole % of Nd formed Nd, Fe-rich ferrihydrite as initial precipitates, which were poorly crystalline. Aging of the Nd-containing ferrihydrite in 0.3 M OH^- at 40°C and at pH 9.2 at 70°C formed Nd-free goethite and Nd-substituted hematite. The abundance of these crystalline phases was related to Nd in the parent solutions. Phase abundance, unit-cell parameters, and peak width were estimated by use of the Rietveld method.

Key Words—Ferrihydrite, Goethite, Hematite, Neodymium, Powder X-ray Diffractometry, Rietveld Refinement, Transmission Electron Microscopy.

INTRODUCTION

In a geological repository for high-level nuclear waste forms, iron minerals will be generated as a result of corrosion of engineered barrier materials and weathering of natural iron-containing minerals. These iron minerals are expected to fix some hazardous radionuclides released from the waste forms, and to retard the migration of these radionuclides in ground water. The freshly formed iron mineral, ferrihydrite, is poorly crystalline, and has a large capacity for sorption and/or incorporation of foreign elements (Sakamoto and Senoo, 1994). Under the redox conditions prevailing near the surface of the earth, ferrihydrite is likely to crystallize into more stable phases, *e.g.,* goethite or hematite (Schwertmann and Murad, 1983). These crystalline phases have a smaller surface area and lower capacity for sorption than the ferrihydrite precursor (Payne *et al.,* 1994). During the crystallization process, an adsorbate may be partially released into ground water. In addition, the crystal structure of iron minerals may be influenced by foreign elements.

In pedogenic environments, iron minerals play an important role in the fixation of foreign anions and cations (Schwertmann and Taylor, 1989). For instance, an aluminum ion (Al^{3+}) can be substituted for Fe^{3+} at the octahedral site of the goethite structure because it has the same valence and a similar ionic radius: 0.0535 nm for $^{vi}Al^{3+}$ and 0.0645 nm for $^{vi}Fe^{3+}$ (Schulze, 1984; Schulze and Schwertmann, 1984, 1987; Shannon, 1976).

Actinide elements such as uranium, neptunium, plutonium, americium (Am), and curium (Cm) have various ionic radii and valences (II to VII), and may be bound to iron minerals by other fixation mechanisms (compared to aluminum). These mechanisms also depend on redox conditions and temperature. However, the number of studies of the fixation mechanisms of these elements and of their modes of incorporation into crystalline iron oxides is limited (Gerth, 1990).

In the present paper, we investigate the effect of neodymium (Nd) on the transformation of ferrihydrite to iron oxides, and the possibility of isomorphous substitution of Nd^{3+} for Fe^{3+} in the goethite or hematite structure. Lanthanide neodymium is used as an inactive substitute for trivalent radioactive actinide elements, because it has a similar chemical behavior. In particular, it is similar in ionic radius in six-fold coordination: 0.0983 nm ($^{vi}Nd^{3+}$), 0.098 nm ($^{vi}Am^{3+}$), and 0.097 nm ($^{vi}Cm^{3+}$) (Shannon, 1976). For this reason, the results of experiments involving Nd may be extrapolated to these actinide elements in their trivalent state.

EXPERIMENTAL METHODS

Preparation

Aqueous solutions (200 mL) of ferric nitrate (0.2 M) and neodymium nitrate (0.2 M) were mixed to attain Nd/(Nd + Fe) mole ratios of 0, 2, 5, 7, 10, 15, 20, and 30%. The mixtures were hydrolyzed by adjusting the pH to ~7.5 with aqueous ammonia. The

† Present address: Department of Environmental Sciences, Japan Atomic Energy Research Institute, Tokai, Naka, Ibaraki 319-1195, Japan.

‡ Present address: Department of Fuel Cycle Safety Research, Japan Atomic Energy Research Institute, Tokai, Naka, Ibaraki 319–1195, Japan.

§ Present address: Interactive Research Center for Science, Tokyo Institute of Technology, O-okayama 2-12-1, Meguro, Tokyo 152-8551, Japan.

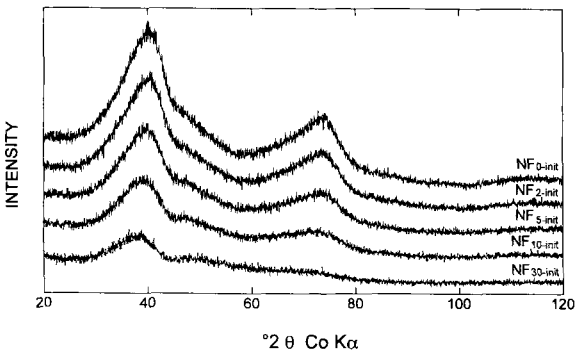

Figure 1. Powder XRD patterns of initial precipitates from Fe- and/or Nd-containing solutions. A label of $NF_{x\text{-init}}$ represents a precipitate from a parent solution having x% of Nd/(Nd + Fe) mole ratio.

mixtures were poured into a dialysis tube, and the resulting precipitates were washed with distilled water in a 1-L beaker at 15°C. The conductivity of the water was measured and the water replaced with freshly-distilled water daily. After dialyzing for 10 d, the conductivity of the wash water became nearly constant. A small portion of the precipitates was freeze-dried.

Deionized water was added to the dialyzed suspension sample to compensate for the volume reduction during the dialysis. This suspension was then divided into two portions. A 2 M solution of sodium hydroxide was added to one portion until the amount of excess OH^- was 0.3 M. This mixture was aged in an oven at 40°C for 10 d. These conditions are favorable for the formation of goethite only. A 0.2 M aqueous solution of sodium nitrate was added to the other portion of the suspension to achieve the ionic strength of 0.1, and the pH of the mixture was adjusted to ~9.2 with aqueous ammonia. This mixture was aged in a polyethylene bottle in a thermostated oven at 70°C for 9 d. Under these conditions, both goethite and hematite form. The resulting precipitates were washed in dialysis tubes at 15°C for 10 d and freeze-dried.

Characterization

The samples were examined using transmission electron microscopy (TEM) (Hitachi, H-800) combined with energy dispersive X-ray spectrometry (EDX) (Kevex, 7000). Before measurement, sediments were ultrasonically dispersed in deionized water, the pH of which was adjusted to ~10.5 with aqueous ammonia. Several drops of the suspension were air-dried on a plastic microgrid.

Samples were also subjected to powder X-ray diffractometry (Rigaku, Geigerflex). X-ray diffraction (XRD) data were collected using CoKα radiation at 40 kV and 20 mA, over the range 20–120 °2θ at a step size of 0.05 °2θ and a counting time per step of 7 s. Known amounts (~10 wt. %) of silicon powder from the National Bureau of Standards (SRM 640b) were added to samples as an internal standard.

The Rietveld method (Rietveld, 1969) was used in the processing of XRD data to estimate phase abundance (Hill and Howard, 1987; Hill, 1993) and unit-cell parameters. The Rietveld program was developed by Wiles and Young (1981) and Howard and Hunter (1997). The background was defined by a four-parameter polynomial in $(2\theta)^n$, where n = −1–2. The diffraction profile was fitted by a pseudo-Voigt function in which the pseudo-Voigt parameter γ_1 was refined. The peak width H was varied in accordance with $H^2 = W + V\tan\theta + U\tan^2\theta$, where W, V, and U are refinable parameters. In addition, unit-cell parameters, scale factor, and positional parameters were refined. The positional parameters for the Fe, O, and H atoms in the goethite unit cell and for the Fe and O atoms in the hematite unit cell were taken from Forsyth *et al.* (1968) and Blake *et al.* (1966), respectively. Site occupancy fractions of individual atoms were fixed.

Absolute weight fractions F_p (wt. %) of crystalline components p were estimated using the following equation: $F_p = F_o(W_p/W_o)100/(100 - F_o)$, where F_o is the weight fraction (wt. %) of the internal standard added, and W_p and W_o are relative weight fractions (wt. %) of the components p and the standard, respectively, determined by the Rietveld-derived method. The weight fraction of ferrihydrite was determined by difference from unity of the sum of the determined absolute weight fractions of all identified crystalline components. The mean coherence length (MCL_{020}) of goethite perpendicular to the (020) plane was estimated from the refined peak width and the instrumental broadening, determined with 20–37-μm size quartz, using the Scherrer formula (Schwertmann and Cornell, 1991).

RESULTS

Initial coprecipitates of Fe and Nd

Figure 1 shows XRD patterns of initial coprecipitates of Fe and Nd. An initial coprecipitate obtained from a parent solution having x% of Nd/(Nd + Fe) mole ratio is termed $NF_{x\text{-init}}$. The pure Fe precipitate ($NF_{0\text{-init}}$) displays broad peaks near 40 and 73 °2θ, which are attributed to 2-line ferrihydrite (Schwertmann and Cornell, 1991). The coprecipitates ($NF_{2\text{-init}}$-$NF_{30\text{-init}}$) also give two broad peaks owing to the 2-line ferrihydrite. The intensities of these two characteristic peaks gradually decrease with increasing Nd/(Nd + Fe) ratio in the parent solutions. The peak near 73 °2θ in $NF_{30\text{-init}}$ is very low in intensity. In addition, the peak positions are gradually shifted to lower angles with increasing Nd/(Nd + Fe) ratio, and the peak near 40 °2θ in $NF_{0\text{-init}}$ is displaced to ~38 °2θ in $NF_{30\text{-init}}$.

In a preliminary experiment using neodymium nitrate alone, hydrolysis products above pH ~ 7.5 con-

https://doi.org/10.1346/CCMN.1999.0470609 Published online by Cambridge University Press

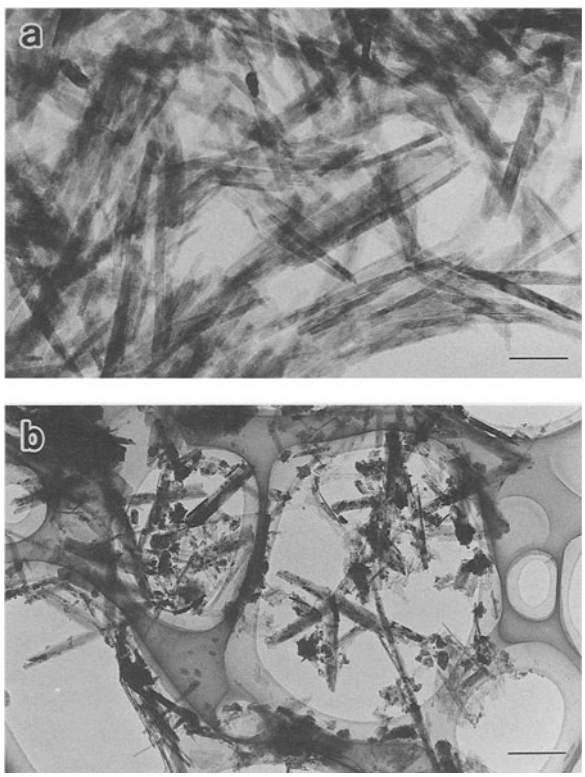

Figure 2. Bright-field TEM images of Nd-containing ferrihydrate aged in 0.3 M OH⁻ at 40°C: (a) 5% and (b) 30% Nd/(Nd + Fe) mole ratios. Scale bars in the images (a) and (b) represent 100 nm and 1 μm, respectively.

sisted mainly of crystalline neodymium hydroxide [$Nd(OH)_3$]. The solubility of $Nd(OH)_3$ in neutral and alkaline solutions is negligibly small (Rao *et al.*, 1996). However, the initial coprecipitates of Fe and Nd were poorly crystalline as shown in Figure 1. These results imply that neodymium was mostly incorporated into the ferrihydrite structure to form a Nd-O/OH-Fe linkage. This is consistent with the peak position at 40 °2θ gradually shifting to lower angles with increasing Nd because the ionic radius of $^{vi}Nd^{3+}$ is larger than that of $^{vi}Fe^{3+}$.

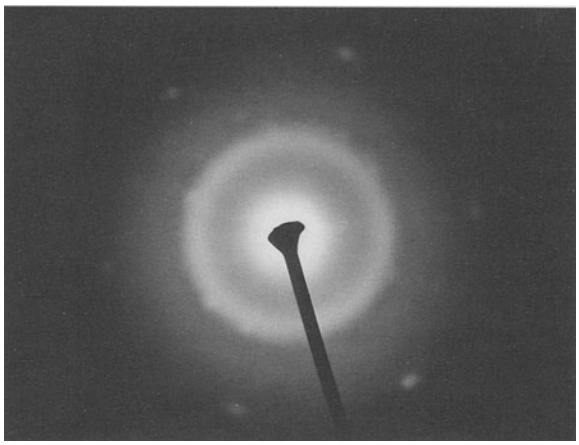

Figure 3. Selected area electron diffraction pattern obtained from an aggregate of small particles in NF_{30-40}.

Aging products in 0.3 M OH⁻ at 40°C

Figure 2 shows TEM images of Nd-containing ferrihydrite aged in 0.3 M OH⁻ at 40°C. An aging product obtained from a parent solution having x% of Nd/(Nd + Fe) mole ratio is termed NF_{x-40}. The morphological observations revealed that the NF_{5-40} sample consisted only of acicular crystals (Figure 2a), which are goethite (see below). The NF_{30-40} sample contained an aggregate of small particles of other phases in addition to the acicular goethite (Figure 2b).

The goethite in NF_{5-40} has a crystal length of ≤500 nm and a width of 10–30 nm (Figure 2a), whereas the goethite in NF_{30-40} has a crystal length of 5 μm at maximum and a width of 100–200 nm (Figure 2b). The MCL_{020} of NF_{5-40} is 14 nm (Table 1) and corresponds well to the width of goethite crystals observed in Figure 2a, whereas the MCL_{020} of NF_{30-40} is 23 nm and much smaller than the crystal width observed in Figure 2b because of the domain character of the goethite. EDX spectra obtained from the goethite crystals in NF_{30-40} showed that the goethites contained only Fe and no Nd.

Figure 3 shows a selected area electron diffraction pattern of the aggregate of small particles shown in

Table 1. Summary of the Rietveld refinement for goethite (Gt) in aging products in 0.3 M OH⁻ at 40°C.

Sample	Gt content (wt. %)	Gt unit cell parameters[1]			MCL_{020} (nm)
		a (nm)	*b* (nm)	*c* (nm)	
NF_{0-40}	76(1)	0.46235(8)	0.9954(1)	0.30244(4)	10
NF_{2-40}	68(1)	0.46240(8)	0.9957(1)	0.30246(4)	11
NF_{5-40}	66(1)	0.46191(7)	0.9960(1)	0.30241(3)	14
NF_{7-40}	57.1(9)	0.46151(7)	0.9961(1)	0.30243(3)	14
NF_{10-40}	45.5(8)	0.46163(8)	0.99610(3)	0.30240(3)	17
NF_{15-40}	27.9(6)	0.4614(1)	0.9958(1)	0.30238(4)	21
NF_{20-40}	22.1(7)	0.4615(2)	0.9958(2)	0.30240(6)	25
NF_{30-40}	16.0(9)	0.4613(3)	0.9960(3)	0.3023(1)	23

[1] Standard deviations in brackets are quoted in units of least significant figure of main value.

https://doi.org/10.1346/CCMN.1999.0470609 Published online by Cambridge University Press

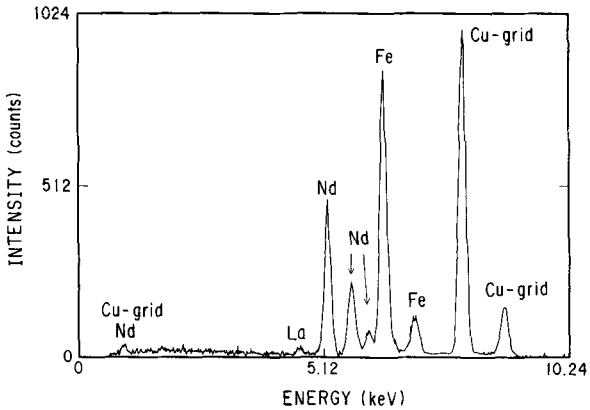

Figure 4. Typical energy spectrum obtained from aggregates of small particles in NF_{30-40}.

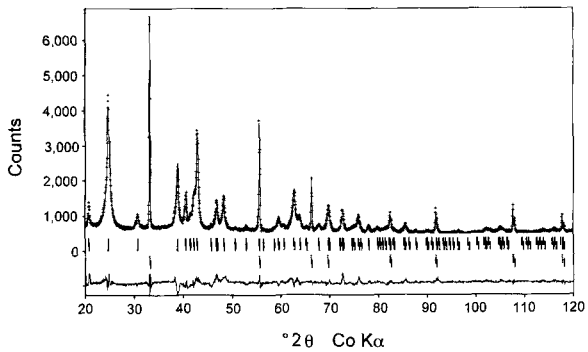

Figure 6. Plot showing the Rietveld method fit to NF_{7-40} in Figure 5. The observed data are indicated by crosses, and the calculated pattern is the continuous line. The short vertical lines below the pattern mark the positions of all Bragg reflections from goethite (top) and silicon (below). The lower curve is the difference between the observed and calculated pattern.

Figure 2b. The pattern indicates that this phase is poorly crystalline. Figure 4 shows a typical energy spectrum from the aggregate, which consisted mainly of Fe and Nd. The aggregates also contained La derived from an impurity in the Nd reagent, apart from Cu due to the microgrid. The *d*-value calculated from the radius of the halo in Figure 3 is ~2.8 Å, and this is consistent with the value of ~2.75 Å obtained from the XRD of $NF_{30\text{-init}}$ (Figure 1).

Figure 5 shows XRD patterns of precipitates aged in 0.3 M OH^- at 40°C for 10 d. All lines in samples of NF_{0-40}-NF_{10-40} are from goethite and the Si standard. In the XRD patterns of NF_{15-40}-NF_{30-40}, however, weak additional reflections at 32.3, 33.7, 37.5, 47.3, and 58.4 °2θ are due to neodymium hydroxides (Roy and McKinstry, 1953).

Figure 6 shows the results of the Rietveld refinement for NF_{7-40}, and Table 1 gives absolute proportion and unit-cell parameters of the goethite. The proportion of goethite decreased with increasing Nd/(Nd + Fe) ratio, indicating the inhibition effect of Nd on the formation of goethite from Nd-containing ferrihydrite. The *b* and *c* values were nearly constant in experiments with Nd, whereas the *a* value slightly decreased with increasing Nd content to 7 mole %, above which it became constant. Schwertmann *et al.* (1985) reported that goethite with smaller crystal width has a greater amount of H_2O in the structure and higher *a* values, although *b* and *c* do not change significantly with crystal width. Therefore, higher *a* values in the present paper are probably related to structural defects and/or site vacancies. These defects and vacancies produce excess OH in the structure (Schwertmann and Stanjek, 1998), because crystal widths, represented by the MCL_{020}, in samples with lower Nd/(Nd + Fe) ratios, are smaller (Table 1).

Aging products at pH 9.2 and 70°C

Figure 7 shows XRD patterns of products aged at pH 9.2 and 70°C for 9 d. The dominant iron oxides are dependent on the Nd/(Nd + Fe) ratio of the parent

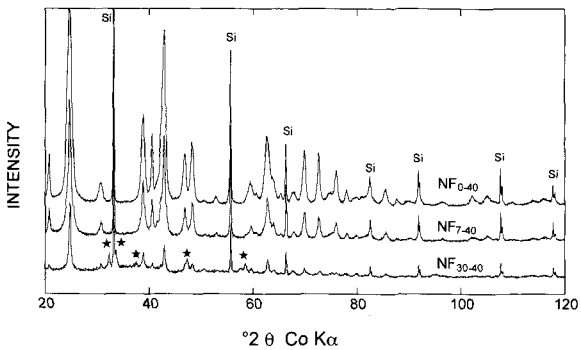

Figure 5. Powder XRD patterns of aging products in 0.3 M OH^- at 40°C. A label of NF_{x-40} represents an aging product from an initial precipitate of $NF_{x\text{-init}}$. All peaks belong to goethite, except those marked Si and ★ are silicon and $Nd(OH)_3$, respectively.

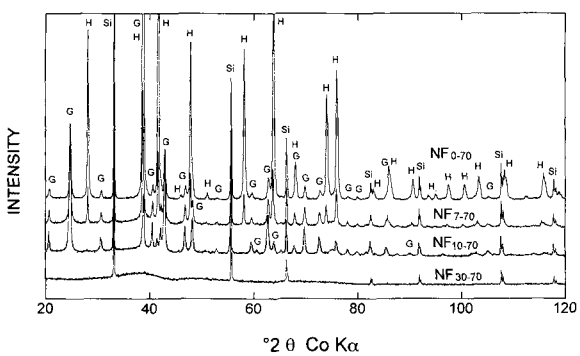

Figure 7. Powder XRD patterns of aging products at pH 9.2 and 70°C. A label of NF_{x-70} represents an aging product from an initial precipitate of $NF_{x\text{-init}}$. The labels G, H, and Si stand for goethite, hematite, and silicon, respectively.

https://doi.org/10.1346/CCMN.1999.0470609 Published online by Cambridge University Press

Table 2. Summary of the Rietveld refinement for hematite (Hm) and goethite (Gt) in aging products at pH 9.2 and 70°C.

Sample	Hm content (wt. %)	Hm unit cell parameters[1]		Gt content (wt. %)	Gt unit cell parameters[1]		
		a (nm)	*c* (nm)		*a* (nm)	*b* (nm)	*c* (nm)
NF_{0-70}	65.3(5)	0.50378(2)	1.37595(4)	12.5(3)	0.46062(7)	0.9968(1)	0.30216(3)
NF_{2-70}	53.4(5)	0.50395(2)	1.37660(4)	19.0(3)	0.46083(5)	0.99654(9)	0.30227(2)
NF_{5-70}	34.0(5)	0.50424(3)	1.37817(5)	20.5(4)	0.46115(6)	0.9964(1)	0.30237(3)
NF_{7-70}	22.4(5)	0.50433(4)	1.37911(8)	31.2(6)	0.46095(5)	0.9965(1)	0.30237(2)
NF_{10-70}	—	—	—	52.9(7)	0.46115(4)	0.99669(6)	0.30240(2)
NF_{15-70}	—	—	—	23.6(7)	0.46143(9)	0.9972(1)	0.30229(4)

[1] Standard deviations in brackets are quoted in units of least significant figure of main value.

solutions. With the Nd/(Nd + Fe) mole ratios of 0–7%, both goethite and hematite are present, whereas only goethite is observed for the Nd/(Nd + Fe) mole ratios of 10–15%. For higher Nd/(Nd + Fe) ratios, poorly crystalline material alone is present. Since the XRD profile of the NF_{30-70} is similar to that of $NF_{30\text{-init}}$ (Figure 1), the poorly crystalline phase is likely Nd-containing ferrihydrite which survived the aging.

The proportion and unit-cell parameters of goethite and hematite are summarized in Table 2. Figure 8 shows the relationship between the proportion of iron oxides and the Nd/(Nd + Fe) ratio of a parent solution. The proportion of hematite decreases with increasing Nd/(Nd + Fe) ratio and is negligibly small at the ratio of ≥10%. On the other hand, the proportion of goethite increases with increasing Nd/(Nd + Fe) ratio (≤10%), and then decreases to zero at 20%. The content of ferrihydrite increases with increasing Nd/(Nd + Fe) ratio and reaches 100 (wt. %) at the ratio of 20%.

Morphology (Figure 9a) as observed by TEM also showed that the NF_{7-70} sample consisted of two phases: one acicular in shape (goethite) and one subrounded (hematite). An electron diffraction pattern (Figure 9b) along the [4$\bar{8}$43] zone axis for the subrounded crystal shows that the phase was hematite. Since hematite in NF_{7-70} contained Nd as well as Fe (Figure 10) and both *a* and *c* for the hematite gradually increase with increasing Nd/(Nd + Fe) ratio (Table 2), the Fe in the hematite structure is probably replaced partly by Nd.

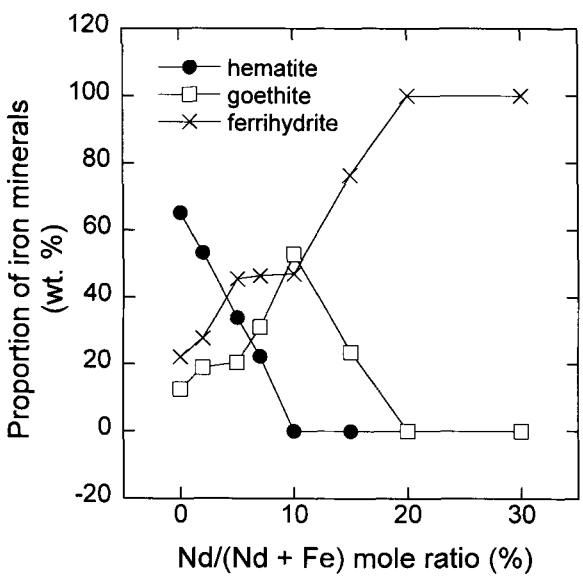

Figure 8. Proportion of iron minerals in aging products at pH 9.2 and 70°C as a function of Nd/(Nd + Fe) ratio in the parent solution.

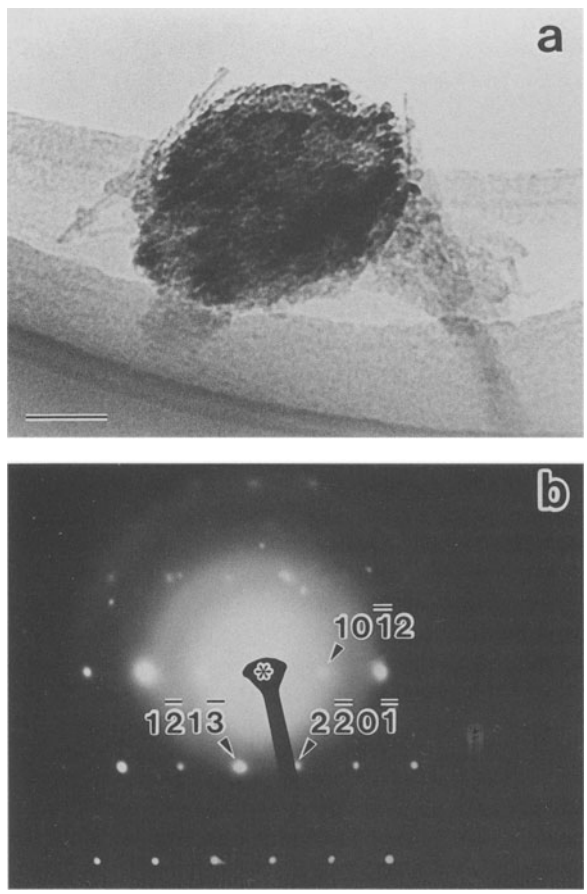

Figure 9. (a) Bright-field TEM image, and (b) selected area electron diffraction pattern (zone axis, [4$\bar{8}$43]) for hematite in an aging product of NF_{7-70} at pH 9.2 and 70°C. The scale bar in the image (a) represents 40 nm.

https://doi.org/10.1346/CCMN.1999.0470609 Published online by Cambridge University Press

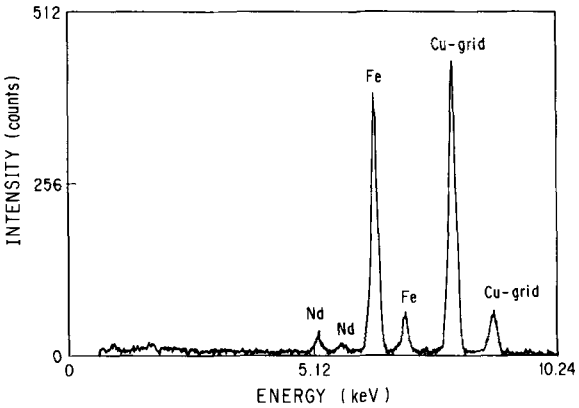

Figure 10. Typical energy spectrum obtained from hematite in the aging product of NF_{7-70} at pH 9.2 and 70°C.

DISCUSSION

Sesquioxides of Nd (Nd_2O_3) occur in two forms, hexagonal (A-type) and cubic (C-type). The hexagonal form is the most common at elevated temperature (Haire and Eyring, 1994). The similarity in the structures of hematite and the A-type Nd_2O_3 favors the formation of the Nd-substituted hematite. In this substitution, the unit cell must expand as shown in Table 2, since the ionic radius of $^{vi}Nd^{3+}$ (0.0983 nm) is greater than that of $^{vi}Fe^{3+}$ (0.0645 nm) (Shannon, 1976).

A decrease in the hematite proportion with increasing Nd/(Nd + Fe) from 0 to 10% (Figure 8) indicates that hematite formation was hindered by Nd. On the other hand, the goethite proportion increased to 10% of Nd/(Nd + Fe) and decreased above 10% (Figure 8). This implies that Nd initially promotes the formation of goethite to 10%, and inhibits goethite formation above 10%. The initial increase in the goethite proportion may be explained by arguing that goethite formed at the expense of hematite. This was suggested for the "competitive" formation mechanism of goethite and hematite (Cornell and Schwertmann, 1996). Because the sum of the goethite and hematite proportion, as determined by subtraction of the ferrihydrite proportion (Figure 8) from 100 (wt. %), tends to decrease with increasing Nd/(Nd + Fe) to 20%, Nd hindered conversion of ferrihydrite, even during the competitive process. The increase in the goethite proportion to 10% of Nd/(Nd + Fe) suggests that the process promoting the formation of goethite would have overcome the inhibition process under these conditions.

The ability of Nd to inhibit goethite and hematite formation may be explained by considering the formation mechanisms of the two oxides. Previous studies suggested that goethite crystallizes through dissolution of ferrihydrite and consecutive precipitation of Fe as goethite, whereas hematite grows through dehydration and/or rearrangement of ferrihydrite (Feitknecht and Michaelis, 1962; Schwertmann and Fischer, 1966; Cornell *et al.*, 1989). The Nd-O/OH-Fe linkage, as stated above, probably suppresses dehydration, internal rearrangement, and dissolution of the Nd-containing ferrihydrite. Therefore, the conversion to goethite and/or hematite is inhibited.

ACKNOWLEDGMENTS

We thank T.E. Payne, Australian Nuclear Science & Technology Organisation, for a critical review of the manuscript. We are also indebted to U. Schwertmann, S. Guggenheim, W.H. Hudnall, and an anonymous reviewer for their critical and useful comments.

REFERENCES

Blake, R.L., Hessevick, R.E., Zoltai, T., and Finger, L.W. (1966) Refinement of the hematite structure. *The American Mineralogist,* **51,** 123–129.

Cornell, R.M. and Schwertmann, U. (1996) *The Iron Oxides.* VCH, Weinheim, 313–347.

Cornell, R.M., Giovanoli, R., and Schneider, W. (1989) Review of the hydrolysis of iron (III) and the crystallization of amorphous iron (III) hydroxide hydrate. *Journal of Chemical Technology and Biotechnology,* **46,** 115–134.

Feitknecht, W. and Michaelis, W. (1962) Uber die Hydrolyse von Eisen (III) perchlorat-Losungen. *Helvetica Chimica Acta,* **45,** 212–224.

Forsyth, J.B., Hedley, I.G., and Johnson, C.E. (1968) The magnetic structure and hyperfine field of goethite (α-FeOOH). *Journal of Physics, C (Proceedings of Physical Society) Series 2,* **1,** 179–188.

Gerth, J. (1990) Unit-cell dimensions of pure and trace metal-associated goethites. *Geochimica et Cosmochimica Acta,* **54,** 363–371.

Haire, R.G. and Eyring, L. (1994) Comparisons of the binary oxides. In *Handbook on the Physics and Chemistry of Rare Earths,* K.A. Gschneidner, L. Eyring, Jr., G.R. Choppin, and G.H. Lander, eds., Elsevier Science, Amsterdam, The Netherlands, 413–505.

Hill, R.J. (1993) Data collection strategies: Fitting the experiment to the need. In *The Rietveld Method,* R.A. Young, ed., Oxford University Press, Oxford, UK, 61–101.

Hill, R.J. and Howard, C.J. (1987) Quantitative phase analysis from neutron powder diffraction data using the Rietveld method. *Journal of Applied Crystallography,* **20,** 467–474.

Howard, C.J. and Hunter, B.A. (1997) A computer program for Rietveld analysis of X-ray and neutron powder diffraction patterns. Australian Nuclear Science and Technology Organization, Lucas Heights Research Laboratories, Menai, New South Wales Australia.

Payne, T.E., Davis, J.A., and Waite, T.D. (1994) Uranium retention by weathered schists—the role of iron minerals. *Radiochimica Acta,* **66/67,** 297–303.

Rao, L., Rai, D., and Felmy, A.R. (1996) Solubility of $Nd(OH)_3(c)$ in 0.1 M NaCl aqueous solution at 25°C and 90°C. *Radiochimica Acta,* **72,** 151–155.

Rietveld, H.M. (1969) A profile refinement method for nuclear and magnetic structures. *Journal of Applied Crystallography,* **2,** 65–71.

Roy, R. and McKinstry, H.A. (1953) Concerning the so-called $Y(OH)_3$-type structures, and the structure of $La(OH)_3$. *Acta Crystallographica,* **6,** 365.

Sakamoto, Y. and Senoo, M. (1994) Redistribution of strontium during crystallization of amorphous ferrihydrite to goethite. *Radioactive Waste Management and Environmental Restoration,* **18,** 265–280.

Schulze, D.G. (1984) The influence of aluminum on iron oxides. VIII. Unit-cell dimensions of Al-substituted goethites

and estimation of Al from them. *Clays and Clay Minerals,* **32,** 36–44.

Schulze, D.G. and Schwertmann, U. (1984) The influence of aluminum on iron oxides: X. Properties of Al-substituted goethites. *Clay Minerals,* **19,** 521–539.

Schulze, D.G. and Schwertmann, U. (1987) The influence of aluminum on iron oxides: XIII. Properties of goethites synthesized in 0.3 M KOH at 25°C. *Clay Minerals,* **22,** 83–92.

Schwertmann, U. and Cornell, R.M. (1991) *Iron Oxides in the Laboratory: Preparation and Characterization.* VCH, Weinheim, 137 pp.

Schwertmann, U. and Fischer, W.R. (1966) Zur Bildung von α-FeOOH und α-Fe_2O_3 aus amorphem Eisen(III)-hydroxid III. *Zeitschrift fur Anorganische und Allgemeine Chemie,* **346,** 137–142.

Schwertmann, U. and Murad, E. (1983) Effect of pH on the formation of goethite and hematite from ferrihydrite. *Clays and Clay Minerals,* **31,** 277–284.

Schwertmann, U. and Stanjek, H. (1998) Stirring effects on properties of Al goethite formed from ferrihydrite. *Clays and Clay Minerals,* **46,** 317–321.

Schwertmann, U. and Taylor, R.M. (1989) Iron oxides. In *Minerals in Soil Environments, 2nd edition,* J.B. Dixon and S.B. Weeds, eds., Soil Science Society of America Book Series 1, Madison, Wisconsin, 379–438.

Schwertmann, U., Cambier, P., and Murad, E. (1985) Properties of goethites of varying crystallinity. *Clays and Clay Minerals,* **33,** 369–378.

Shannon, R.D. (1976) Revised effective ionic radii and systematic studies of interatomic distances in halides and chalcogenides. *Acta Crystallographica,* **A32,** 751–767.

Wiles, D.B. and Young, R.A. (1981) A new computer program for Rietveld analysis of X-ray powder diffraction patterns. *Journal of Applied Crystallography,* **14,** 149–151.

E-mail of corresponding author: nagano@sparclt.tokai.jaeri.go.jp

(Received 3 April 1998; accepted 15 May 1999; Ms. 98-045)